J. Fluid Mech. (1977), *vol.* 82, *part* 2, *pp.* 371–387
Printed in Great Britain

Unsteady flows in a semi-infinite contracting or expanding pipe

By SHIGEO UCHIDA AND HIROSHI AOKI
Department of Aeronautical Engineering, Nagoya University,
Chikusa-Ku, Nagoya 464, Japan

(Received 28 July 1976)

Physiological pumps produce flows by alternate contraction and expansion of the vessel. When muscles start to squeeze its wall the valve at the upstream end is closed and that at the downstream end is opened, and the fluid is pumped out in the downstream direction. These systems can be modelled by a semi-infinite pipe with one end closed by a compliant membrane which prevents only axial motion of the fluid, leaving radial motion completely unrestricted. In the present paper an exact similar solution of the Navier–Stokes equation for unsteady flow is a semi-infinite contracting or expanding circular pipe is calculated and reveals the following characteristics of this type of flow. In a contracting pipe the effects of viscosity are limited to a thin boundary layer attached to the wall, which becomes thinner for higher Reynolds numbers. In an expanding pipe the flow adjacent to the wall is highly retarded and eventually reverses at Reynolds numbers above a critical value. The pressure gradient along the axis of pipe is favourable for a contracting wall, while it is adverse for an expanding wall in most cases. These solutions are valid down to the state of a completely collapsed pipe, since the nonlinearity is retained in full. The results of the present theory may be applied to the unsteady flow produced by a certain class of forced contractions and expansions of a valved vein or a thin bronchial tube.

1. Introduction

The main part of the cardiovascular pump is a valved vessel. When the blood in the left ventricle is being forced by systole into the aorta, the mitral valve is closed while the atrioventricular valve is open. At this stage the left ventricle forms a vessel with one end closed.

Considering the high Reynolds number, of order 5000, for the ejection of blood into the aorta, Jones (1969, 1970) proposed a mathematical model for unsteady flow of inviscid fluid in such a vessel. Very little is known so far about unsteady flows of viscous fluid produced by contraction of the walls of a vessel with one end closed.

With regard to the unsteady flow produced in a vessel of infinite length by pulsatile wall deformations, extensive work has been done on peristaltic pumping by many authors such as Fung & Yih (1968), Shapiro, Jaffrin & Weinberg (1969) and others referred to in the comprehensive papers by Jaffrin & Shapiro (1971) and by Lighthill (1972). Fung & Yih (1968) indicate that peristalsis may be involved in the flow through small blood vessels. Previous investigations on peristalsis mostly concern the progressive wave motion through an infinite valveless tube.

A vein of medium size also has a valve system. When it contracts the valve at the upstream end is closed and that at the downstream end is open. In such a vessel or a tube with one end closed the contents are ejected into the adjoining section mainly by the simple contraction of the tube diameter, even though the peristalsis, if any, may help to transport the contents. By cooperating with motions of valve a vein with a valve system can act as a local pumping station powered by the action of muscles.

A similar situation can be seen in the unsteady air flow through a thin bronchial tube, which has no valve but is closed at one end by lung alveoli. Since the tube is terminated by numerous air cells, the condition at the closed end may not be simple.

In the present paper the blood vessel, closed at one end by a valve, or the thin bronchial tube is modelled by a semi-infinite circular pipe with one end closed by an idealized compliant membrane which prevents only axial motion, leaving radial motion completely unrestricted. Unsteady flows produced by a single contraction or expansion of the wall are then calculated. The end condition can be satisfied by using an infinite pipe divided into two parts by a compliant membrane at the origin stretched perpendicular to the axis of the pipe. The fluid flow is symmetrical about this membrane, therefore the axial velocity vanishes.

Assuming that the radius of the pipe is a function only of time, i.e. $a = a(t)$, a solution of the Navier–Stokes equation similar with respect to axial distance from the closed end can be obtained. Denoting axial and radial distance by x and r, respectively, the stream function is found to be proportional to x times a function $F(\eta, t)$, where $\eta = r/a$. By introducing the non-dimensional parameter $\alpha(t) = \dot{a}a/\nu$, in which $\dot{a} = da/dt$ is the velocity of the wall and ν is the kinematic viscosity, the differential equation for $F(\eta, t)$ can be written in terms of $\alpha(t)$ and η only. If we assume further that the function F is a function only of η and that α is a constant parameter, the similar solution for the stream function may be calculated from the differential equation for $F(\eta)$, which contains α as a constant parameter.

The present solution is valid for contraction down to complete collapse of the pipe to zero diameter and for expansion up to infinite diameter, since the nonlinearity is retained in full. Numerical results for the velocity components, the pressure distribution and the shearing stress on the wall are also presented. Though the present similar solution requires a particular class of imposed wall motions, it may be applicable to a certain type of forced contraction or expansion of a valved vein or a thin bronchial tube.

2. Fundamental relations

Unsteady flow of an incompressible viscous fluid through a semi-infinite circular pipe whose radius varies with time is considered. A section of such a pipe with a contracting wall is shown in figure 1. The pipe is closed at $x = 0$ by an elastic membrane which prevents axial motion but is fully compliant to radial motion produced by the wall. This situation may easily be achieved by making the flow symmetrical about the plane $x = 0$, as shown in the figure.

Referring to cylindrical co-ordinates (x, r, θ) and denoting the velocity components in the axial and radial directions by u and v respectively, axisymmetric unsteady flow

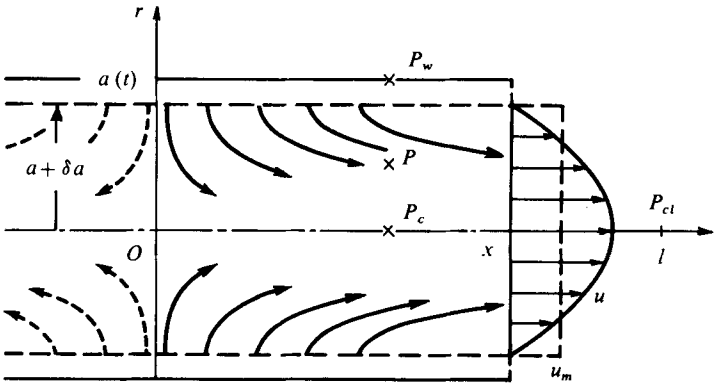

FIGURE 1. Flow patterns in a contracting pipe.

is governed by the following equations of continuity and of motion:

$$u_x + v_r + v/r = 0, \tag{1}$$

$$u_t + uu_x + vu_r = -p_x/\rho + \nu(u_{xx} + u_{rr} + u_r/r), \tag{2}$$

$$v_t + uv_x + vv_r = -p_r/\rho + \nu(v_{xx} + v_{rr} + v_r/r - v/r^2). \tag{3}$$

The wall of the pipe moves only in the radial direction and its radius is assumed to be a function of time only. The radial velocity of fluid at the wall, denoted by v_w, is equal to the wall velocity $da/dt = \dot{a}$. The boundary conditions are therefore

$$\left.\begin{aligned} u = 0, \quad v = v_w = \dot{a} \quad \text{at} \quad r = a(t), \\ u_r = 0, \quad v = 0 \quad \text{at} \quad r = 0 \end{aligned}\right\} \tag{4}$$

and

$$u = 0 \quad \text{at} \quad x = 0, \tag{5}$$

where v is left free.

The flow field becomes greatly simplified in the present circumstances. The volume flow past a section x is supplied by the fluid which was contained in the now diminished volume of pipe between $x = 0$ and x. Thus the mean flow velocity u_m is given by

$$u_m(x, t) = -2x\dot{a}/a, \tag{6}$$

which indicates that u_m is proportional to x.

In order to satisfy the equation of continuity identically, the Stokes stream function ψ defined by

$$u = \psi_r/r, \quad v = -\psi_x/r \tag{7}$$

is introduced. Eliminating the pressure from the equations of motion gives the vorticity equation

$$\zeta_t + u\zeta_x + v\zeta_r - v\zeta/r = \nu(\zeta_{xx} + \zeta_{rr} + \zeta_r/r - \zeta/r^2), \tag{8}$$

where $\zeta = v_x - u_r = -[(\psi_x/r)_x + (\psi_r/r)_r]$ is the vorticity component normal to the meridian plane. Substitution of (7) into (8) gives a differential equation for ψ.

3. Similar solution with respect to x

Since the variation of the wall radius is independent of x and the flow has no particular length scale in the x direction, a similar solution with respect to x can be expected. Because the boundary conditions are imposed on $r/a = 0$ and 1, a non-dimensional variable proportional to r/a is first introduced, and a similar solution of the form $\psi = x^m f(a) F(\eta, t)$, where $\eta = Ar/a$, is examined.

It is easily found that this expression gives a mean axial velocity proportional to x^m. Comparison with (6) thus gives $m = 1$. It is noted that in this case $u_{xx} = v_x = 0$. Substituting these expressions into the vorticity equation (8) and comparing the dimensions of the inertial terms, proportional to xf^2/a^5, and the viscous terms, proportional to $xf\nu/a^5$, we obtain $f(a) = \nu$. In order to simplify the formulation A is taken to be unity; this will be discussed further in the next section.

Consequently the similar solution is of the form

$$\psi = \nu x F(\eta, t), \quad \eta = r/a. \tag{9}$$

The axial and radial velocity components are, respectively,

$$u = (\nu x/a^2)(F_\eta/\eta), \quad v = -(\nu/a)(F/\eta). \tag{10}$$

The boundary condition (5) is found to be satisfied automatically. Since v is independent of x in this particular configuration, the vorticity is simply $\zeta = -u_r$, and (3) reduces to $p_{rx} = 0$. It is found that the characteristics of the present flow are simplified by these relations.

Substituting $\zeta = -u_r$ and $v/r = -u_x - v_r$, from continuity, into the vorticity equation (8), we have

$$[\nu(u_{xx} + u_{rr} + u_r/r) - (u_t + uu_x + vu_r)]_r = 0. \tag{11}$$

The same expression can also be obtained by direct calculation of $p_{xr} = 0$ from (2). Substitution of (10) into (11) gives the differential equation for F as

$$[G(\eta, t)]_\eta = 0, \tag{12}$$

$$G(\eta, t) = \left(\frac{F_\eta}{\eta}\right)_{\eta\eta} + \left(\frac{1}{\eta} + \frac{F}{\eta} + \alpha\eta\right)\left(\frac{F_\eta}{\eta}\right)_\eta - \left(\frac{F_\eta}{\eta} - 2\alpha\right)\frac{F_\eta}{\eta} - \frac{a^2}{\nu}\frac{F_{\eta t}}{\eta}, \tag{13}$$

where α is defined by using $\dot{a}$ in place of da/dt:

$$\alpha(t) = \dot{a}a/\nu. \tag{14}$$

The transformed expressions for the boundary conditions given by (4) are

$$\left.\begin{aligned} &F/\eta = 0, \quad (F_\eta/\eta)_\eta = 0 \quad \text{at} \quad \eta = 0, \\ &F/\eta = -\alpha, \quad F_\eta/\eta = 0 \quad \text{at} \quad \eta = 1. \end{aligned}\right\} \tag{15}$$

It is easily confirmed that the mean velocity calculated from (10) and (15) coincides with (6).

On substituting (10) into (2) and (3), the pressure gradients can be calculated from

$$p_x = (\rho\nu^2 x/a^4)\,G, \tag{16}$$

$$p_r = \rho\frac{\nu^2}{a^3}\left\{-\left[\left(\frac{F}{\eta}\right)_\eta + \left(\frac{1}{\eta}+\frac{1}{2}\frac{F}{\eta}+\alpha\eta\right)\frac{F}{\eta}\right]_\eta + \frac{a^2}{\nu}\frac{F_t}{\eta}\right\}, \tag{17}$$

where p_r can be replaced by p_η/a. The shearing stress is given by

$$\tau = \mu\left(\frac{\partial v}{\partial x}+\frac{\partial u}{\partial r}\right) = \frac{\rho\nu^2 x}{a^3}\left(\frac{F_\eta}{\eta}\right)_\eta. \tag{18}$$

4. Similar solution with respect to space and time

In order to analyse the fundamental properties of the present flow, a full solution similar in both space and time which preserves the nonlinear characteristics of the problem is studied in this section.

Such a similar solution can be obtained by assuming $F_{\eta t} = 0$ and $\alpha =$ constant in (13), which means that the function F is a function only of η containing α as a constant parameter. The value of α is taken as its initial value:

$$\dot{a}a/\nu = \alpha = \dot{a}_0 a_0/\nu, \tag{19}$$

where a_0 and $\dot{a}_0 = (da/dt)_0$ are the initial values of the radius and of its expansion rate, respectively. Contracting and expanding pipes thus have $\alpha < 0$ and $\alpha > 0$ respectively. The parameter $|\alpha|$ is the Reynolds number which represents the dynamical scale of the present motion. Integrating (19), it is found that for the present similar solution the radius of the pipe should vary in time according to

$$a/a_0 = [1+2\alpha(\nu t/a_0^2)]^{\frac{1}{2}}, \tag{20}$$

and we have the rate of change

$$v_w/(v_w)_{t=0} = \dot{a}/\dot{a}_0 = [1+2\alpha(\nu t/a_0^2)]^{-\frac{1}{2}}. \tag{21}$$

Some numerical examples of a/a_0 are shown in figure 2.

It is noticed that the value of the stream function on the wall, which is denoted by ψ_w, is a linear function of x:

$$\psi_w = \nu x F(1) = -\nu x\alpha. \tag{22}$$

The differential equation for $F(\eta)$ is written with a prime in place of $d/d\eta$,

$$[G(\eta)]' = 0, \tag{23}$$

and is integrated as follows:

$$G(\eta) = \left(\frac{F'}{\eta}\right)'' + \left(\frac{1}{\eta}+\frac{F}{\eta}+\alpha\eta\right)\left(\frac{F'}{\eta}\right)' - \left(\frac{F'}{\eta}-2\alpha\right)\frac{F'}{\eta} = K, \tag{24}$$

where K is a constant. The boundary conditions are

$$\left.\begin{aligned} &F/\eta = 0, \quad (F'/\eta)' = 0 \quad \text{at} \quad \eta = 0,\\ &F/\eta = -\alpha, \quad F'/\eta = 0 \quad \text{at} \quad \eta = 1. \end{aligned}\right\} \tag{25}$$

The condition $u = 0$ at $x = 0$ can be satisfied automatically, provided that F'/η is finite.

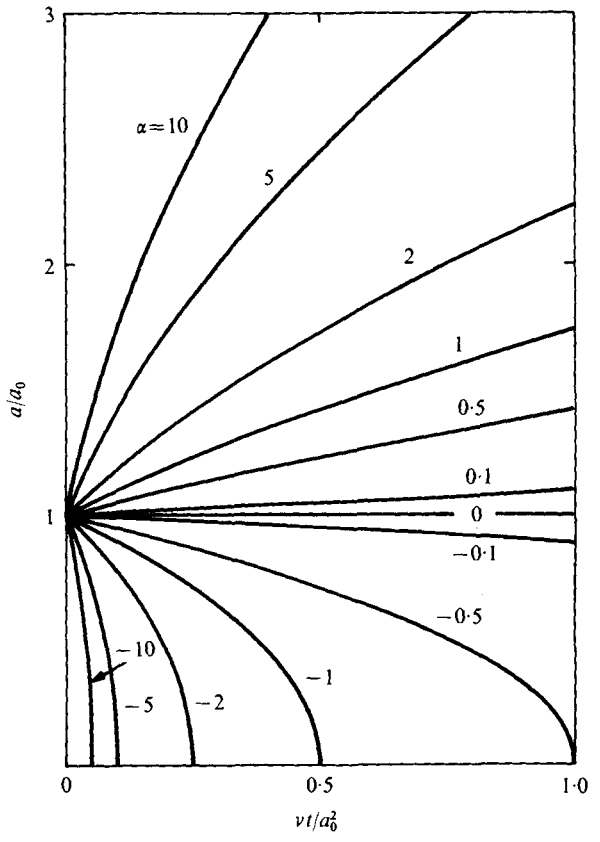

FIGURE 2. Variation of the wall radius with time.

As mentioned in the previous section we choose the independent variable defined by $\eta = r/a$. Other forms of variable, for instance $\xi = |\alpha|^{\frac{1}{2}}\eta$, may be used in place of η to transform (24) into a simpler expression which does not contain α explicitly. However, the boundary condition at the wall becomes rather complicated: $F/\xi = -|\alpha|^{\frac{1}{2}}$ at $\xi = |\alpha|^{\frac{1}{2}}$. Thus we choose $\eta = r/a$ as the independent variable.

The function F is calculated by numerical integration of (24). Since the present form of (24) is singular at the origin, F is expanded in a power series

$$F = b_0 + b_1\eta + b_2\eta^2 + b_3\eta^3 + \ldots \tag{26}$$

in the region close to the origin. Substituting this expression into (24) and (25), we have

$$b_0 = b_1 = b_3 = \ldots = b_{2n+1} = 0. \tag{27}$$

The remaining coefficients may be expressed as functions of b_2 and K:

$$b_4 = \tfrac{1}{16}[K + 4(b_2 - \alpha)\, b_2], \quad b_6 = \tfrac{1}{12}(b_2 - 2\alpha)\, b_4, \quad b_8 = -\tfrac{1}{72}(9\alpha b_6 - 2b_4^2),$$

$$b_{2n+4} = -\Bigg\{[(2n-4)\, b_2 + (2n+2)\,\alpha]\,(2n+2)\, b_{2n+2} + \sum_{m=1}^{n-1} (2n-2-4m)\,(2n+2-2m)\, b_{2m+2}\, b_{2n+2-2m}\Bigg\} \Big/ (2n+2)^2(2n+4) \quad \text{for} \quad n \geqslant 2. \tag{28}$$

α	K	$(F'/\eta)_{\eta=0}$	$(F'')_{\eta=1}$
−10·0	−1267	26·90	−175·36
−5·0	−369·7	14·60	−69·23
−1·0	−29·93	3·620	−9·788
−0·1	−1·744	0·3944	−0·8192
0	0	0	0
0·1	1·451	−0·4055	0·7792
1·0	−1·107	−4·839	5·291
1·2	−7·281	−6·289	5·335
1·4	−17·13	−8·072	4·528
1·6	−35·73	−10·84	1·697
1·67	−54·75	−13·33	−2·156

TABLE 1. Numerical values of the constant K and of the functions at the boundary.

Assuming values of b_2 and K, the function F is calculated from this power series from $\eta = 0$ to $\eta = 0{\cdot}01$, where the calculation is continued by numerical integration by the Runge–Kutta–Gill method up to $\eta = 1$. The coefficients b_2 and K are determined to satisfy boundary conditions (25) at $\eta = 1$. Examples of numerical values of K etc. are shown in table 1.

When the function F has been calculated, non-dimensional expressions for ψ, u_m and the velocity components are obtained from

$$\psi/(\nu a_0) = (x/a_0)\,F, \tag{29}$$

$$\frac{u_m}{\nu/a_0} = -2\alpha\left(\frac{a}{a_0}\right)^{-2}\frac{x}{a_0} = \frac{-2\alpha}{1+2\alpha(\nu t/a_0^2)}\frac{x}{a_0}, \tag{30}$$

$$u/u_m = -(2\alpha)^{-1}(F'/\eta), \tag{31}$$

$$v/v_w = v/\dot{a} = -\alpha^{-1}(F/\eta), \tag{32}$$

where $\dot{a}$ is the expansion rate of the wall radius and is given by

$$\dot{a}(\nu/a_0)^{-1} = \alpha(a/a_0)^{-1}, \quad \text{or} \quad \dot{a}/\dot{a}_0 = (a/a_0)^{-1}. \tag{33}$$

Some examples of the non-dimensional form of the stream function or F,

$$\psi/\psi_w = F(\eta)/F(1) = -F/\alpha, \tag{34}$$

are given in figure 3.

Typical flow patterns for contracting and expanding pipes are shown in figures 4(*a*) and (*b*) respectively. It is found that the streamlines for an expanding tube are more concentrated in the central region on account of retardation in the wall region. In the other half of the pipe ($x < 0$) the flow patterns are symmetrical to those in $x > 0$.

The absolute value of the mean velocity increases with time for a contracting pipe ($\alpha < 0$), while it decreases for an expanding pipe ($\alpha > 0$), as shown in figure 5. Numerical examples of axial velocity distributions referred to the mean velocity are shown in figure 6. It is found that the velocity distribution is fairly monotonic for a contracting pipe, and that the effects of viscosity are limited to a thin boundary layer attached to the wall, which becomes thinner for higher values of the Reynolds number defined by

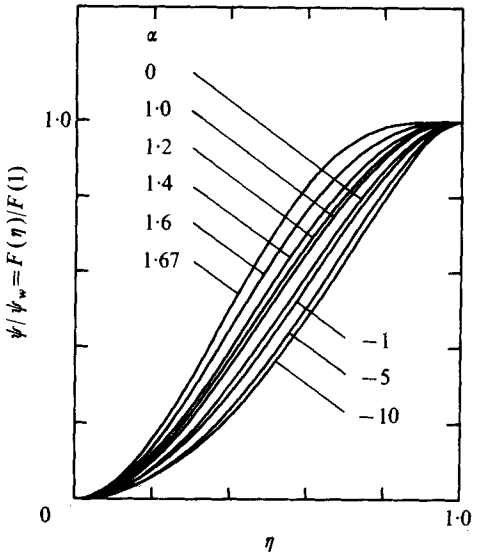

FIGURE 3. Stream function ψ and the function F.

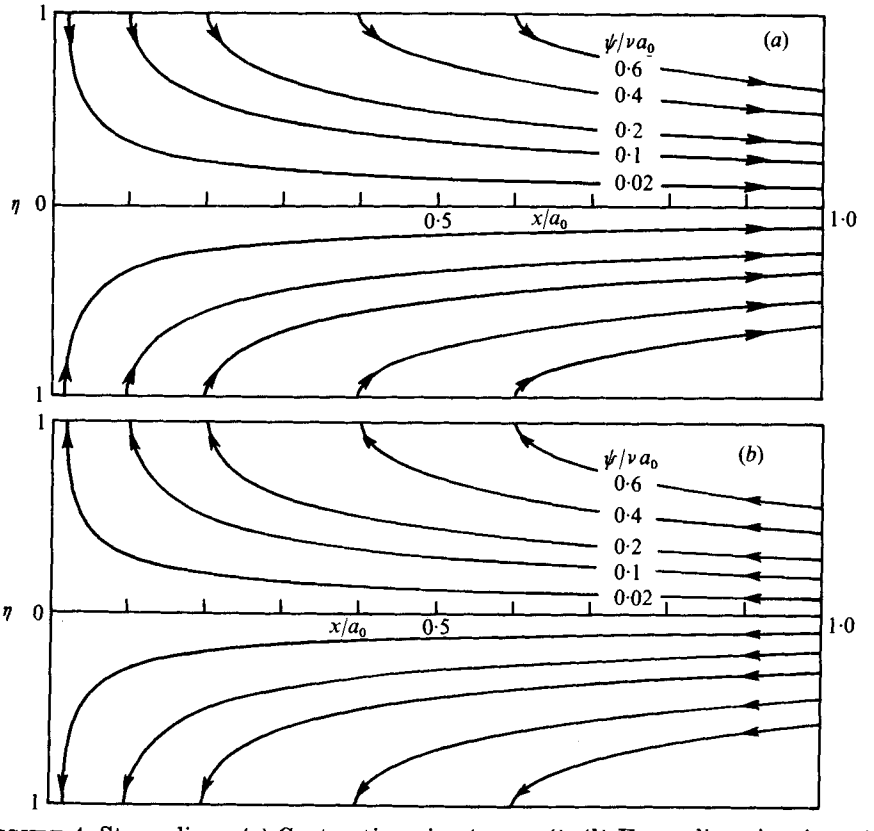

FIGURE 4. Streamlines. (*a*) Contracting pipe ($\alpha = -1$). (*b*) Expanding pipe ($\alpha = 1$).

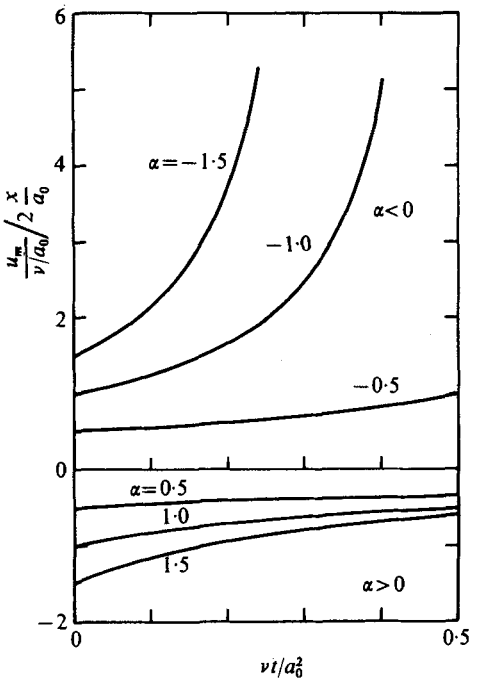

FIGURE 5. Time variation of the mean axial velocity.

$R_e = |\alpha| = |\dot{a}_0 a_0/\nu|$. The velocity distributions for an expanding pipe contain higher harmonics in case of high Reynolds number. The flow adjacent to the wall is highly retarded, and eventually reverse flow occurs in the wall region for Reynolds numbers above a critical value of $\alpha = 1{\cdot}644$. In the limit of low Reynolds number, the velocity distribution approaches a parabolic distribution for both $\alpha < 0$ and $\alpha > 0$.

Distributions of radial velocity referred to $v_w = \dot{a}$ are shown in figure 7. On moving away from the wall along a streamline, the magnitude of the velocity increases, and because of this its radial component also increases at first before falling to zero at the centre of the pipe.

When reverse flow occurs in the wall region of an expanding pipe intense deformations of the flow produce a high maximum value of v/v_w.

Regarding the pressure gradients, we have $p_{xr} = p_{rx} = 0$ from (16) and (17), since G = constant and $F_t = 0$. Hence pressure distributions at a fixed instant can be integrated separately over η and x. The transformed version of (17), given by

$$p_\eta = -\rho(\nu^2/a^2)\,[(F''/\eta) + \tfrac{1}{2}(F/\eta)^2 + \alpha F]', \tag{35}$$

can be integrated along a radius at a constant x. Denoting the pressure on the axis by $p_c(x,t)$, we have

$$\frac{p-p_c}{\rho\nu^2/a_0^2} = -\left[\frac{F''}{\eta} + \frac{1}{2}\left(\frac{F}{\eta}\right)^2 + \alpha F - \left(\frac{F''}{\eta}\right)_{\eta=0}\right]\left(\frac{a}{a_0}\right)^{-2}. \tag{36}$$

Numerical values of $(F''/\eta)_{\eta=0}$ for various α's are given in table 1. It is noted that the pressure difference $p - p_c$ is a function of η and t only, and is independent of x. Two

(a)

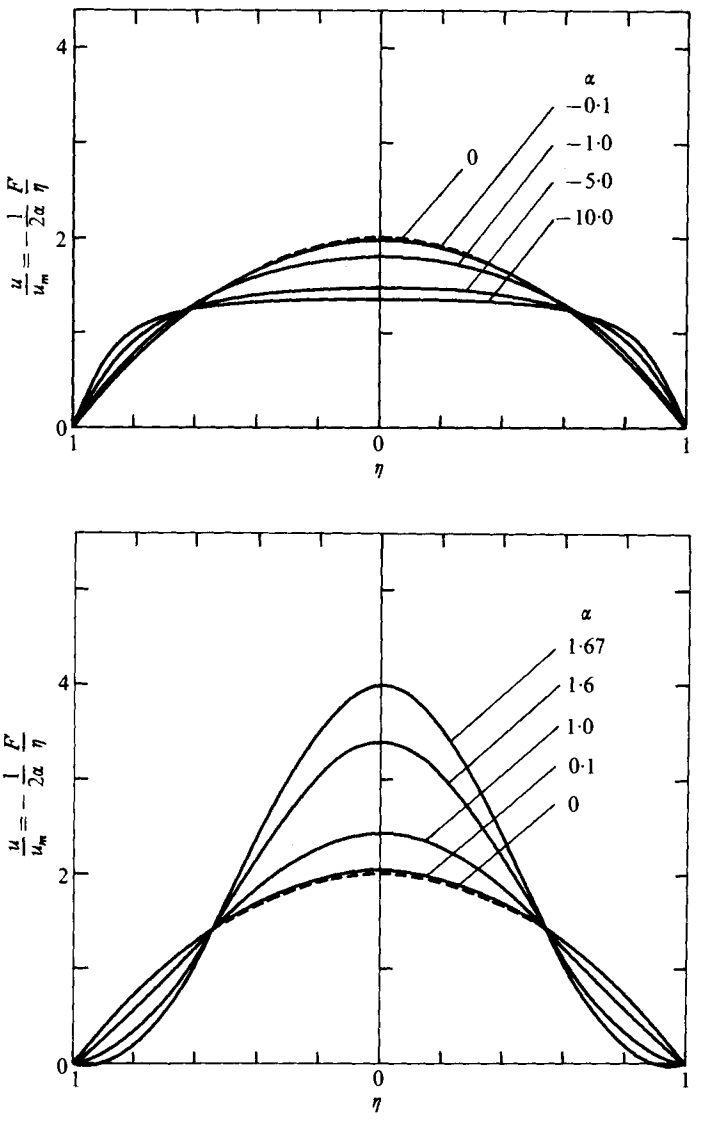

FIGURE 6. Distributions of axial velocity. (*a*) Contracting pipes. (*b*) Expanding pipes.

examples are shown in figure 8. In a contracting pipe the pressure at the wall is higher than that at the centre and vice versa in an expanding pipe. The pressure difference between the wall and the centre is also constant in every section, and is given by

$$\frac{p_w - p_c}{\rho\nu^2/a_0^2} = \left[\frac{\alpha^2}{2} + \left(\frac{F'}{\eta}\right)_{\eta=0}\right]\left(\frac{a}{a_0}\right)^{-2}. \tag{37}$$

By integrating (16) the pressure distribution along a line η = constant is calculated as

$$\frac{p}{\rho\nu^2/a_0^2} = \frac{K}{2}\frac{x^2}{a_0^2}\left(\frac{a}{a_0}\right)^{-4} + C. \tag{38}$$

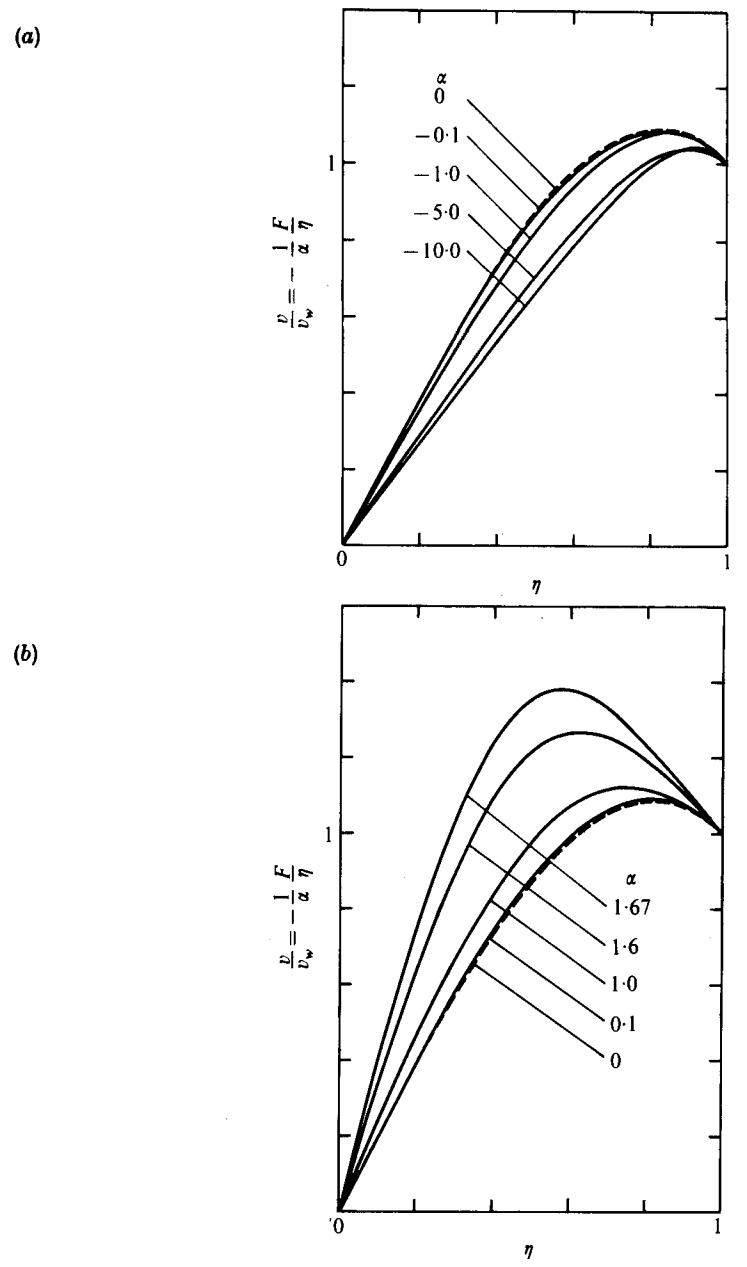

FIGURE 7. Distributions of radial velocity. (*a*) Contracting pipes. (*b*) Expanding pipes.

We have the following pressure distribution along the axis:

$$\frac{p_c - p_{cl}}{\rho\nu^2/a_0^2} = \frac{K}{2}\frac{x^2 - l^2}{a_0^2}\left(\frac{a}{a_0}\right)^{-4}, \tag{39}$$

where p_{cl} is the reference pressure on the axis at a fixed point $x = l$.

The variation of the pressure at the centre with time and space is shown in figure 9.

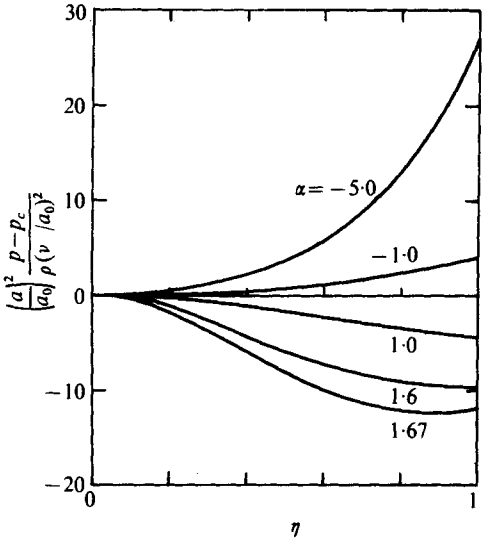

FIGURE 8. Radial pressure distributions.

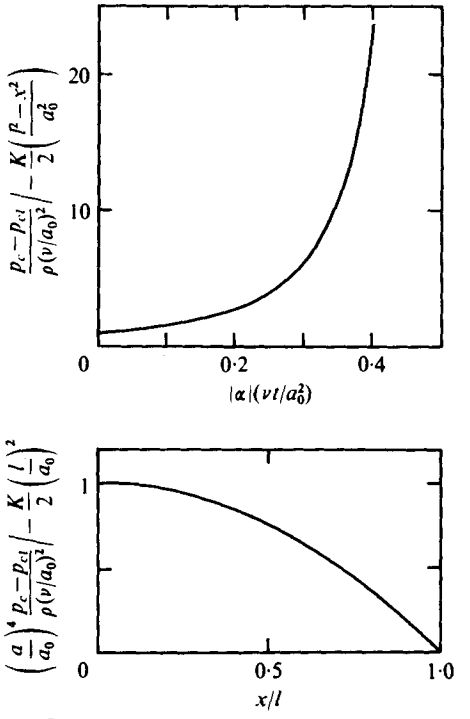

FIGURE 9(*a*). For legend see facing page.

(*b*)

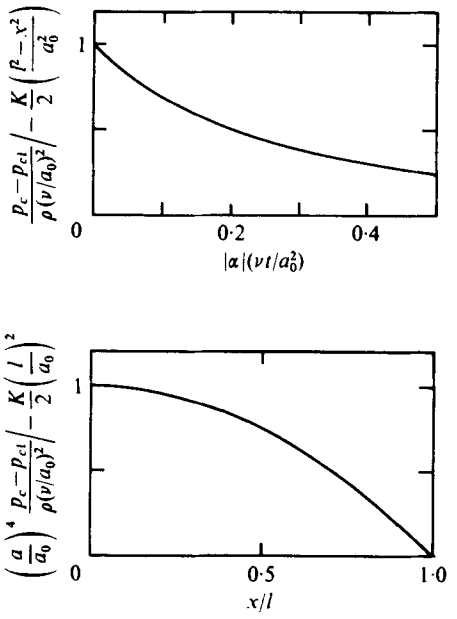

FIGURE 9. Time variation and distribution of pressure along the axis of the pipe. (*a*) Contracting pipe. (*b*) Expanding pipe.

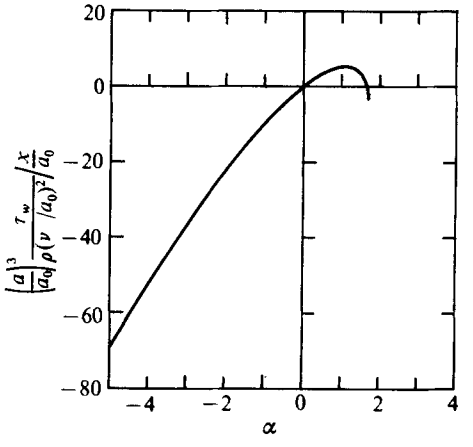

FIGURE 10. Shearing stress along the wall.

Since $K < 0$ in most cases, it is found that the pressure difference $p_c - p_{cl}$ increases with time for a contracting pipe and decreases for an expanding pipe. It is also interesting that $p_c - p_{cl}$ has the highest value at the origin for $K < 0$. This means that fluid flows under a favourable pressure gradient in a contracting pipe and that the pressure gradient is adverse in an expanding pipe except for $0 < \alpha < 0{\cdot}95$.

By combining (36) and (39), the pressure at an arbitrary point is calculated to be

$$\frac{p-p_{cl}}{\rho\nu^2/a_0^2} = -\left[\frac{F'}{\eta}+\frac{1}{2}\left(\frac{F}{\eta}\right)^2+\alpha F-\left(\frac{F'}{\eta}\right)_{\eta=0}\right]\left(\frac{a}{a_0}\right)^{-2}-\frac{K}{2}\frac{l^2-x^2}{a_0^2}\left(\frac{a}{a_0}\right)^{-4}. \tag{40}$$

Substituting boundary values at $\eta = 1$ into (40), we obtain the wall pressure p_w as follows:

$$\frac{p_w - p_{cl}}{\rho\nu^2/a_0^2} = \left[\frac{\alpha^2}{2} + \left(\frac{F'}{\eta}\right)_{\eta=0}\right]\left(\frac{a}{a_0}\right)^{-2} - \frac{K}{2}\frac{l^2 - x^2}{a_0^2}\left(\frac{a}{a_0}\right)^{-4}. \tag{41}$$

The necessary power for the external forces which balance the wall pressure can be calculated as

$$P = 2\pi a \int_0^l p_w(-da/dt)\,dx. \tag{42}$$

Since the wall does not move in the axial direction, it is noted that the shearing stress along the wall does not contribute to the work done by external forces. Integrating (42), the non-dimensional form of P is given by

$$\frac{P}{\rho\nu^3/a_0} = -2\pi\alpha\left\{\frac{p_{cl}}{\rho\nu^2/a_0^2}\frac{l}{a_0} + \left[\frac{\alpha^2}{2} + \left(\frac{F'}{\eta}\right)_{\eta=0}\right]\frac{l}{a_0}\left(\frac{a}{a_0}\right)^{-2} - \frac{K}{3}\left(\frac{l}{a_0}\right)^3\left(\frac{a}{a_0}\right)^{-4}\right\}, \tag{43}$$

where $a/a_0 = 1 + 2\alpha(\nu t/a_0^2)$.

The work done during the time interval $t = 0$ to t is calculated as

$$W = \int_0^t P\,dt.$$

Substituting $[(F'/\eta)']_{\eta=1} = (F'')_{\eta=1}$ into (18), the shearing stress along the wall is given by

$$\frac{\tau_w}{\rho\nu^2/a_0^2} = (F'')_{\eta=1}\frac{x}{a_0}\left(\frac{a}{a_0}\right)^{-3}. \tag{44}$$

It is noticed that τ_w is proportional to the axial distance from the origin. The non-dimensional form of the frictional drag D_f acting on the part of tube between $x = 0$ and l is

$$\frac{D_f}{\rho\nu^2} = \frac{2\pi}{\rho\nu^2}\int_0^l \tau_w a\,dx = \pi(F'')_{\eta=1}\left(\frac{l}{a_0}\right)^2\left(\frac{a}{a_0}\right)^{-2}. \tag{45}$$

Values of

$$(F'')_{\eta=1} = \frac{(a/a_0)^3}{x/a_0}\frac{\tau_w}{\rho\nu^2/a_0^2} = \frac{1}{\pi}\frac{(a/a_0)^2}{(l/a_0)^2}\frac{D_f}{\rho\nu^2} \tag{46}$$

for various α are shown in table 1 and in figure 10, where the sign of τ_w depends on its definition (18). It is noted that τ_w changes sign at $\alpha = 1{\cdot}644$ because reverse flow begins in the wall region.

5. Solution for a low Reynolds number

The previous solution shows that the effects of viscosity are indicated by the parameter $|\alpha|$, i.e. the Reynolds number for the present flow. The solution for a low Reynolds number can therefore be obtained by expanding variables in power series in α.

The radius of the pipe and its rate of change are found by expanding (20) and (21) respectively:

$$\frac{a}{a_0} = 1 + \alpha\left(\frac{\nu t}{a_0^2}\right) - \tfrac{1}{2}\alpha^2\left(\frac{\nu t}{a_0^2}\right)^2 + \tfrac{1}{2}\alpha^3\left(\frac{\nu t}{a_0^2}\right)^3 + \ldots, \tag{47}$$

$$\frac{\dot{a}}{\dot{a}_0} = 1 - \alpha\left(\frac{\nu t}{a_0^2}\right) + \tfrac{3}{2}\alpha^2\left(\frac{\nu t}{a_0^2}\right)^2 - \tfrac{5}{2}\alpha^3\left(\frac{\nu t}{a_0^2}\right)^3 + \ldots. \tag{48}$$

Since the orders of magnitude of u/u_m and v/v_w in (31) and (32) are unity even for a vanishingly small value of α, the power-series expansion of the function F and accordingly that of the constant K may start with an α^1 term. They can be assumed to have the forms

$$F(\eta) = \alpha F_1(\eta) + \alpha^2 F_2(\eta) + \ldots + \alpha^n F_n(\eta) + \ldots, \tag{49}$$

$$K = \alpha K_1 + \alpha^2 K_2 + \ldots + \alpha^n K_n + \ldots. \tag{50}$$

Substituting these expressions into (24) and (25) gives differential equations for the F_n,

$$\left(\frac{F_1'}{\eta}\right)'' + \frac{1}{\eta}\left(\frac{F_1'}{\eta}\right)' = K_1, \tag{51}$$

$$\left(\frac{F_2'}{\eta}\right)'' + \frac{1}{\eta}\left(\frac{F_2'}{\eta}\right)' + \left(\frac{F_1}{\eta} + \eta\right)\left(\frac{F_1'}{\eta}\right)' - \left(\frac{F_1'}{\eta} - 2\right)\frac{F_1'}{\eta} = K_2, \tag{52}$$

$$\left(\frac{F_3'}{\eta}\right)'' + \frac{1}{\eta}\left(\frac{F_3'}{\eta}\right)' + \left(\frac{F_1}{\eta} + \eta\right)\left(\frac{F_2'}{\eta}\right)' - 2\left(\frac{F_1'}{\eta} - 1\right)\frac{F_2'}{\eta} + \left(\frac{F_1'}{\eta}\right)'\frac{F_2}{\eta} = K_3, \tag{53}$$

etc., and the boundary conditions

$$\left.\begin{aligned} F_1/\eta = 0, \quad (F_1'/\eta)' = 0 \quad \text{at} \quad \eta = 0, \\ F_1 = -1, \qquad F_1' = 0 \quad \text{at} \quad \eta = 1, \end{aligned}\right\} \tag{54}$$

$$\left.\begin{aligned} F_n/\eta = 0, \quad (F_n'/\eta)' = 0 \quad \text{at} \quad \eta = 0 \\ F_n = 0, \qquad F_n' = 0 \quad \text{at} \quad \eta = 1 \end{aligned}\right\} \text{for} \quad n \geqslant 2. \tag{55}$$

These equations can be easily integrated, resulting in

$$F_1 = -2\eta^2 + \eta^4, \tag{56}$$

$$F_2 = -\tfrac{5}{18}\eta^2 + \tfrac{7}{12}\eta^4 - \tfrac{1}{3}\eta^6 + \tfrac{1}{36}\eta^8, \tag{57}$$

$$F_3 = -\tfrac{1057}{10800}\eta^2 + \tfrac{271}{1080}\eta^4 - \tfrac{47}{216}\eta^6 + \tfrac{2}{27}\eta^8 - \tfrac{7}{720}\eta^{10} + \tfrac{1}{5400}\eta^{12}, \tag{58}$$

etc., and values of the K_n may also be determined:

$$K_1 = 16, \quad K_2 = -\tfrac{44}{3}, \quad K_3 = -\tfrac{208}{135}, \text{ etc.} \tag{59}$$

The constant K is therefore given by

$$K = 16\alpha - \tfrac{44}{3}\alpha^2 - \tfrac{208}{135}\alpha^3 + \ldots. \tag{60}$$

The stream function is given by

$$\psi/(\nu a_0) = (x/a_0)\,[\alpha F_1 + \alpha^2 F_2 + \alpha^3 F_3 + \ldots]. \tag{61}$$

The velocity components are calculated from

$$\begin{aligned} u/u_m &= -\tfrac{1}{2}[(F_1'/\eta) + \alpha(F_2'/\eta) + \alpha^2(F_3'/\eta) + \ldots] \\ &= 2(1-\eta^2) + \alpha[\tfrac{5}{18} - \tfrac{7}{6}\eta^2 + \eta^4 - \tfrac{1}{9}\eta^6] \\ &\quad + \alpha^2[\tfrac{1057}{10800} - \tfrac{271}{540}\eta^2 + \tfrac{47}{72}\eta^4 - \tfrac{8}{27}\eta^6 + \tfrac{7}{144}\eta^8 - \tfrac{1}{900}\eta^{10}] + \ldots, \end{aligned} \tag{62}$$

$$\begin{aligned} v/v_w &= -(F_1/\eta) - \alpha(F_2/\eta) - \alpha^2(F_3/\eta) - \ldots \\ &= (2\eta - \eta^3) + \alpha[\tfrac{5}{18}\eta - \tfrac{7}{12}\eta^3 + \tfrac{1}{3}\eta^5 - \tfrac{1}{36}\eta^7] \\ &\quad + \alpha^2[\tfrac{1057}{10800}\eta - \tfrac{271}{1080}\eta^3 + \tfrac{47}{216}\eta^5 - \tfrac{2}{27}\eta^7 + \tfrac{7}{720}\eta^9 - \tfrac{1}{5400}\eta^{11}] + \ldots. \end{aligned} \tag{63}$$

In the limit $\alpha \to 0$, it is found that the distribution of axial velocity is parabolic as in Hagen–Poiseuille flow. The radial velocity always has the maximum value

$$v_{\max}/v_w = \tfrac{4}{3}(\tfrac{2}{3})^{\frac{1}{2}} = 1{\cdot}0887 \quad \text{at} \quad \eta = (\tfrac{2}{3})^{\frac{1}{2}} = 0{\cdot}81650$$

even in the limit $\alpha \to 0$.

The radial pressure distribution at a fixed x is given by

$$\frac{p-p_c}{\rho\nu^2/a_0^2} = [\alpha(-4\eta^2)+\alpha^2(-\tfrac{7}{3}\eta^2+3\eta^4-\tfrac{13}{18}\eta^6) + \alpha^3(-\tfrac{173}{135}\eta^2+\tfrac{13}{6}\eta^4-\tfrac{163}{108}\eta^6+\tfrac{11}{24}\eta^8-\tfrac{3}{100}\eta^{10})+\ldots]\left(\frac{a}{a_0}\right)^{-2}. \tag{64}$$

The pressure difference between the wall and the centre is calculated by putting $\eta = 1$ in (64):

$$\frac{p_w-p_c}{\rho\nu^2/a_0^2} = [-4\alpha-\tfrac{1}{18}\alpha^2-\tfrac{1057}{5400}\alpha^3+\ldots]\left(\frac{a}{a_0}\right)^{-2}. \tag{65}$$

The pressure distribution along the axis is given by

$$\frac{p_c-p_{cl}}{\rho\nu^2/a_0^2} = [-8\alpha+\tfrac{22}{3}\alpha^2+\tfrac{104}{135}\alpha^3+\ldots]\frac{l^2-x^2}{a_0^2}\left(\frac{a}{a_0}\right)^{-4}, \tag{66}$$

where p_{cl} is the reference pressure at a fixed point $x = l$, $r = 0$. The pressure at an arbitrary point is obtained by adding (64) and (66).

The necessary power for the external forces driving the present motion is calculated as

$$\frac{P}{\rho\nu^3/a_0} = -2\pi\alpha\frac{p_{cl}}{\rho\nu^2/a_0^2}\frac{l}{a_0}+2\pi[4\alpha^2+\tfrac{1}{18}\alpha^3+\ldots]\frac{l}{a_0}\left(\frac{a}{a_0}\right)^{-2} + 2\pi[\tfrac{16}{3}\alpha^2-\tfrac{44}{9}\alpha^3-\ldots]\left(\frac{l}{a_0}\right)^3\left(\frac{a}{a_0}\right)^{-4}. \tag{67}$$

The shearing stress along the wall and the frictional drag between $x = 0$ and l are given by (44) and (45) with

$$(F'')_{\eta=1} = 8\alpha-2\alpha^2-\tfrac{56}{135}\alpha^3+\ldots. \tag{68}$$

6. Concluding remarks

A similar solution for the unsteady flows produced by a single contraction or expansion of the wall of a semi-infinite circular pipe has been investigated with special attention to the nonlinear characteristics of such unsteady flows. This flow model is motivated by physiological pumping like that in the left ventricle, in valved veins and in thin bronchial tubes. In many real organs regular contraction and expansion are repeated, being accompanied by the switching of valves.

The time history of the diameter of the left ventricle is not a simple sinusoidal curve but is fairly close to a saw-tooth wave. According to the measurements by Gould *et al.* (1972), the contraction rate of the middle section of the wall of the left ventricle is $\dot{a}_0 \approx -2$ cm/s and its mean semi-axis is $a_0 \approx 3{\cdot}6$ cm. Using $\nu = 0{\cdot}035$ cm^2/s for blood, we have quite a high absolute value of α: $\alpha \approx -200$. Since the left ventricle is not a cylindrical tube but has the shape of a bulb and since its pulsatile motion can not be separated into a single contraction or expansion, the present calculation may not be applicable directly to the flow in a left ventricle. The fundamental mechanism of the

flow in part of systole or diastole, however, can be deduced from the present analysis. For instance, it is noted that the effect of viscosity is limited to a thin layer attached to the wall surface at such a high value $|\alpha| = 200$.

In a forced contraction or expansion, time variation of the diameters of valved veins and thin bronchial tubes can be achieved by the action of voluntary muscles or by control of the external pressure. In a practical sense even a single contraction, a stop or a single expansion is possible. When a valved vein of initial radius $a_0 = 0{\cdot}35$ cm is contracted at an initial rate $\dot{a}_0 = 0{\cdot}2$ cm/s, we have $\alpha = 2$ for blood with $\nu = 0{\cdot}035$ cm^2/s. In a thin bronchial tube with $a_0 = 0{\cdot}15$ cm contracting at an initial rate $\dot{a}_0 = 0{\cdot}1$ cm/s, $\alpha = 0{\cdot}1$ is obtained by the use of $\nu = 0{\cdot}15$ cm^2/s for air. These vessels are fairly long circular tubes, and therefore the present theory can be applied for a forced contraction or expansion similar to that given by (20) and (21).

The results of the present analysis may be summarized as follows.

(i) The effects of viscosity are indicated by the Reynolds number $|\alpha| = |\dot{a}_0 a_0/\nu|$.

(ii) The axial velocity is proportional to x, i.e. to the distance from the closed end, while the radial velocity is independent of x.

(iii) At a very low Reynolds number the distribution of axial velocity is parabolic.

(iv) In the flow due to a contracting wall the effects of viscosity are confined to a boundary layer attached to the wall which becomes thinner for higher Reynolds number.

(v) In the case of an expanding wall the flow adjacent to the wall is highly retarded, and ultimately reverse flow occurs at $\alpha \geqslant 1{\cdot}644$. The distribution of axial velocity contains higher harmonics.

(vi) The distribution of radial velocity has a maximum between the axis and the wall.

(vii) The pressure at the wall is higher than that at the centre for contracting pipes, and vice versa for expanding ones.

(viii) The pressure gradient along the axis is favourable for contracting pipes and adverse for expanding pipes except for $0 < \alpha < 0{\cdot}95$.

(ix) The shearing stress on the wall rapidly increases in absolute value with increasing $|\alpha|$ for contracting pipes, while its value is small for expanding pipes and changes sign beyond $\alpha = 1{\cdot}644$.

The authors acknowledge T. Nawa and the Computing Center of Nagoya University for their help in the numerical computations. Part of the financial aid was provided by the Research Institute of Environmental Medicine, Nagoya University.

REFERENCES

Fung, Y. C. & Yih, C. S. 1968 *J. Appl. Mech.* **35**, 669.

Gould, P., Ghista, D., Brombolich, L. & Mirsky, I. 1972 *J. Biomech.* **5**, 521.

Jaffrin, M. Y. & Shapiro, A. H. 1971 *Ann. Rev. Fluid Mech.* **3**, 13.

Jones, R. T. 1969 *Ann. Rev. Fluid Mech.* **1**, 223.

Jones, R. T. 1970 *Med. Biol. Engng* **8**, 45.

Lighthill, M. J. 1972 *J. Fluid Mech.* **52**, 475.

Shapiro, A. H., Jaffrin, M. Y. & Weinberg, S. L. 1969 *J. Fluid Mech.* **37**, 799.